Physics of Plasmas ARTICLE scitation.org/journal/php

Self-oscillations in an over-injected electron diode – Experiment and analysis

Cite as: Phys. Plasmas **26**, 033113 (2019); doi: 10.1063/1.5087708
Submitted: 3 January 2019 · Accepted: 26 February 2019 ·
Published Online: 19 March 2019

M. Siman-Tov, J. G. Leopold, and Ya. E. Krasik

AFFILIATIONS

Physics Department, Technion, Israel Institute of Technology, Haifa 3200003, Israel

ABSTRACT

An experimental setup to demonstrate a recent scheme [Leopold *et al.*, Phys. Plasmas **24**, 073116 (2017)] to persistently over-inject a vacuum electron diode so that it self-oscillates in the GHz-frequency range and releases a periodic train of electron bunches is described. We present simulations in which we account for the finite rise time of the voltage accelerating electrons from a finite radius cylindrical thermionic cathode and finite grid electrode transparency, which make the experiment different from the original theoretical scheme. It was found that these experimental conditions do affect the expected results but a self-oscillating behavior is still possible. Our experimental results so far indicate the presence of the self-oscillatory behavior, but because the cathode used emits from a few hot-spots rather than uniformly, the beam current modulations are different from those obtained in the simulations.

I. INTRODUCTION

The 1D steady state Child-Langmuir (CL) model of electron emission for an infinite plane cathode (C)–anode (A) gap developed more than a hundred years ago is still considered to be the physical foundation for all high-current vacuum electron guns operating in the space-charge-limited (SCL) emission mode. Such guns are used in many applications from accelerators to high power microwave sources. The theoretical and experimental advances in SCL emission and flow since this pioneering work have been recently reviewed in detail.[1]

If a C–A gap diode is over-injected, that is, more current than that allowed by SCL emission is introduced into it, a virtual cathode (VC) develops near the cathode. If over-injection persists, the current flowing in the diode will oscillate in time. This happens because the VC periodically releases electron bunches with current amplitudes exceeding the SCL value of the diode current, allowing temporarily more charge to be present in the diode gap than that allowed by steady state SCL flow. This behavior was predicted by the pioneering work of Birdsall and Bridges[2,3] and led to the development of vircators. However, the direct observation of a virtual cathode, periodically self-releasing electron bunches, has not been observed because continuous over-injection has not been realized. Electron bunches released by a VC have so far been directly observed in the research described in Refs. 4–7. In these experiments, to over-inject a C-A gap, a pulse of an intense laser, shorter than the time-of-flight of electrons in this gap, is focused on the surface of a thermionic cathode operating at the SCL. The laser pulse enhances the electron emission by local photo-injection. However, periodic bunch emission is obtained only by the periodic application of the laser pulses. In another experiment, self-bunching was observed in the rf photo-injector of the ELSA FEL when the electron pulse charge was too high.[8] Even though a self-oscillating VC producing periodic electron bunches has not been realized so far, it has been suggested that such a scheme is possible by continuously shining a laser over a cathode surface and that this can be used in important applications.[9] Periodic electron bunches traversing a single cavity can replace a continuous beam interacting with a periodic cavity slow wave structure in a microwave source.

In a recent paper,[10] we have suggested a different way to over-inject a diode persistently and produce a beam consisting of periodic electron bunches. This idea was demonstrated by PIC simulations which triggered an experimental effort to reproduce these predictions. The understanding of the difficulties introduced by the experimental setup chosen has though revealed important limitations not considered earlier. For the experiment, three important factors need to be accounted for. First, the cathode, which is a finite area cylindrical dispenser cathode, is not a uniform current density electron source. Second, the voltage applied on the cathode is a pulse with a non-negligible rise-time, and third, electrons impacting grids, though highly transparent, release a non-negligible current of secondary electrons which can change the space charge in the gaps and consequently the potential distribution in the gap. These differences introduce a complex dynamical behavior which is interesting on its own and affects the scheme suggested in Ref. 10. In this paper, we present the

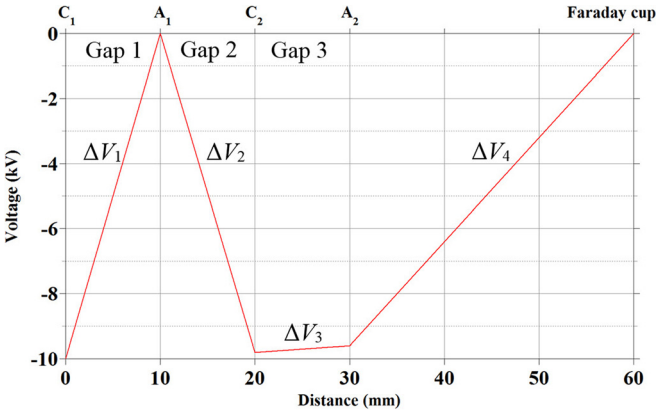

FIG. 1. The potential distribution in an experimental setup prior to electron injection where $\Delta V_1 = 10$ kV, $\Delta V_2 = -9.8$ kV, $\Delta V_3 = 0.1$ kV, and $\Delta V_4 = 9.7$ kV.

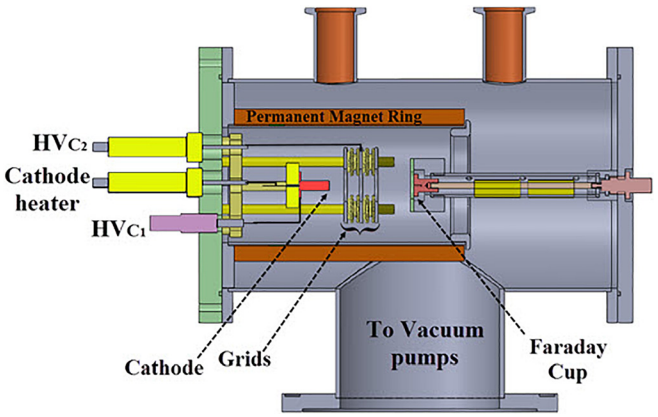

FIG. 2. A sketch of the experimental vacuum chamber and the location of the dispenser cathode, the various grids, the separating insulators, and the Faraday cup.

analysis of the experiment, and our predicted results for this experimental scheme. We also present our experimental results which so far do not directly reproduce our analysis, and we explain the reasons for this behavior.

II. THE EXPERIMENTAL SETUP

The potential distribution in the absence of the electron beam in the experimental arrangement expected to result in diode over-injection is sketched in Fig. 1. A constant axial magnetic field is applied along the entire structure to suppress transverse electron motion. In Ref. 10, we assumed that a finite circular cathode C_1, part of an infinite conducting area, biased negatively relative to a grounded anode A_1, emits electrons with a uniform current density distribution across the beam's cross-sectional area. This electron beam, with current significantly below the SCL of the C_1–A_1 gap, is accelerated in this gap by an applied potential difference ΔV_1 and decelerated in the A_1–C_2 gap by a potential difference ΔV_2 formed by the negatively biased cathode C_2. The deceleration though ($\Delta V_1 > |\Delta V_2|$) leaves the electrons with sufficient energy so that space charge accumulation near C_2 does not form a VC and no current is being reflected in the triode C_1–A_1–C_2 as it would be in a reflex triode. Thus, the entire current of this electron beam is injected into the C_2–A_2 gap, and for a sufficiently high acceleration (ΔV_3), this beam is transmitted downstream towards a grounded Faraday cup (FC) unperturbed. However, when ΔV_3 is sufficiently low, the current transmitted from the triode to the C_2–A_2 gap can become higher than the SCL in this gap. This leads to the formation of a VC in front of the electrode C_2 in the C_2–A_2 gap which releases part of its charge downstream towards the FC and also reflects part of the charge upstream into the triode. The current which returns towards C_1 forms a second VC there which suppresses temporarily the electron emission from the cathode until sufficient current is released by the VC towards the anode A_1. This process becomes periodic, and as long as the cathode C_1 operates continuously, bunches of electrons are released from C_2 downstream, while the charge in the triode C_1-A_1-C_2 oscillates. We showed[10] that since this behavior is controlled by the potential difference ΔV_3, the C_2–A_2 gap can be considered a "diode" which releases electron bunches periodically when over-injected, but that the release frequency depends on the reflection period in the triode. In Ref. 10, we assumed that A_1, C_2, and A_2 were fully transparent.

The experimental setup to realize this approach for generating a high-frequency modulated electron beam is seen in Fig. 2. The cathode chosen is a Ba impregnated Tungsten dispenser cathode (Heatwave model 101439), with a circular emitting surface of radius 3.175 mm, which, when heated to 1200 °C, is expected to emit a 1 A radially distributed uniform electron beam. The Mo grids A_1, C_2, and A_2 are 94% transparent. The permanent magnets are three Neodymium rings (N52) supplying a uniform axial magnetic field of 0.54 T in the volume where the cathode, the grid electrodes, and the FC are placed. During the operation of the thermionic emitter, the temperature of the magnets does not exceed 100 °C which is significantly lower than their

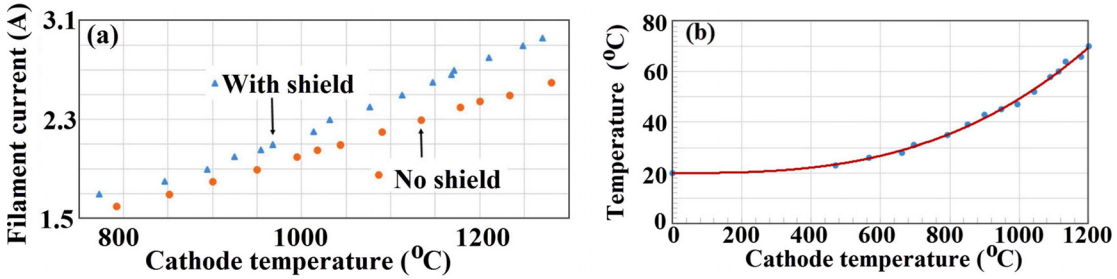

FIG. 3. (a) The dependence of the temperature of the thermionic emitter surface as a function of heater current. (b) The background temperature inside the experimental chamber at a distance of 62 mm from the emitter surface as a function of heater temperature.

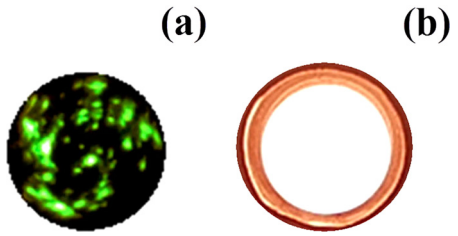

FIG. 4. (a) Electron beam pattern at 1270 °C. (b) The glow of the cathode at 1200 °C.

Curie temperature (∼310 °C). The entire electrode structure is separated by Lava insulators and placed in a stainless steel chamber where the residual pressure was kept at $\sim 10^{-5}$ Pa by turbo- and scroll pumps. A Blumlein pulse generator based on two coaxial RG78 cables and triggered by a gas spark gap switch was designed and used to supply the thermionic emitter with a −10 kV, more than 300 ns long, and ∼50 ns rise time pulse. To decrease the rise time of the voltage to ∼20 ns, an additional sharpening self-breakdown gas spark gap switch was added at the input to the emitter. To decouple the high voltage pulse and the dc power supply of the thermionic cathode heater, an LC filter of a few mH inductance and electrolyte capacitors was used. Adjustable dc voltage power supplies with stored capacitors were used to supply the bias voltages of C_2 and A_2. The form and amplitude of the voltage applied to the cathode C_1 were controlled by a high voltage Tektronix voltage divider, and the dc voltages at the grids C_2 and A_2 were measured by Fluke voltage dividers. The grounded low-inductance Faraday cup measured the transmitted electron current. The waveforms of the applied voltage and electron current were measured by a digitizing oscilloscope DPO 7354C with a bandwidth of 3 GHz.

While setting up this experiment, we realized some difficulties which will affect the expected electron beam dynamics and the experimental results which are presented in Sec. III.

III. EXPERIMENTAL RESULTS

Electron emission was not detected unless the cathode was heated above the maximum temperature of 1200 °C recommended by the cathode manufacturer. To reduce the heat loss and the operating temperature, a specially designed shield was added. The temperature at the surface of the thermionic emitter was measured using a PYRO MICRO-THERM pyrometer (The Pyrometer Instrument Company, accurate to ±0.5 °C), placed at a distance of ∼180 cm from the cathode surface. One can see that the addition of the heat shield allows one to achieve the same emitter surface temperature for 26% less heater power [Fig. 3(a)].

The emission properties of the dispenser cathode C_1 were studied with grids A_1, C_2, and A_2 grounded. The electron beam current was registered by the FC placed at a distance of 62 mm from the cathode surface. For a voltage pulse with amplitudes within 6–15 kV, electron emission starts only when the temperature of the emitter surface exceeds 1200 °C, and it reaches its maximum expected value of ∼1 A.

In order to test the extent of the heat transport from the hot cathode to the grids, the FC, the surrounding magnets, and other supporting structures, the temperature inside the chamber at a distance of 62 mm from the cathode surface was measured using a calibrated thermocouple probe [Fig. 3(b)]. The background temperature does not exceed 70 °C, which is far below the temperature range which can cause the evaporation of atoms from the surface of parts placed inside the experimental chamber.

The cross-sectional uniformity of the emitted electron beam was tested using a Phosphor P43 screen. The screen was covered with a 40 nm Al layer and placed on a glass substrate covered by a second Al layer. The decay time of the light emitted by the P43 phosphor screen is 50–100 ns. The screen was placed at a distance of ∼60 mm from the emitter surface. The magnetized electron beam produces a fluorescence pattern which is registered by an open shutter digital camera. The three grounded 94% transparency Mo grids are placed between the cathode and the screen. Electron beam patterns were obtained for the different values of emission surface temperatures and different accelerating voltages (6–12 kV). The electron beam pattern appears only when the emitter surface temperature exceeds 1150 °C. Increasing the emitter temperature or the amplitude of the accelerating voltage leads to the increase in the light intensity. However, in all these measurements, we found that the light emission is far from uniform and can be defined as spotty [Fig. 4(a)]. At the same time, the direct light emission from the hot cathode [Fig. 4(b)] suggests that the surface temperature is uniform.

Such a spotty electron beam can significantly influence the expected beam modulations, the dynamics of which strongly depends on the dynamics of the space-charge distribution within the entire structure of electrodes. Nevertheless, we attempted to perform these experiments with the existing dispenser cathode. We also observed that the hot spot locations do not change considerably from pulse to pulse and with temperature or voltage. This indicates that the cathode has mostly distinct emission spots not uniformly distributed across the emitter surface.

For grounded A1, C2, and A2 ($\Delta V_1 = 10$ kV and $\Delta V_2 = \Delta V_3 = 0$), we obtain the results shown in Fig. 5. The electron beam current rises to its maximum value of 1 A soon after the voltage is switched on before it reaches its maximum value of ∼10 kV, which signifies that the thermionic emitter operates in a temperature-limited mode. The current is quite stable, which means that even though the cathode is spotty, it emits a constant current.

Next, a dc decelerating voltage is applied on grid C_2 ($\Delta V_2 = -9$ kV), while A_1 and A_2 are grounded. In Fig. 6, one can see waveforms of the voltage ΔV_1 and the electron beam current collected at

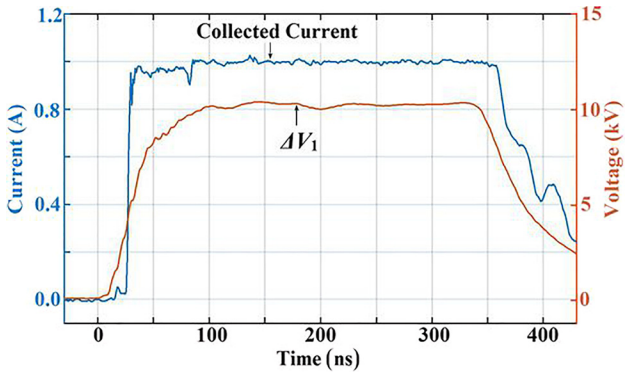

FIG. 5. The time dependence of the voltage ΔV_1 in the C_1-A_1 gap and the current collected on the FC for $\Delta V_2 = \Delta V_3 = 0$.

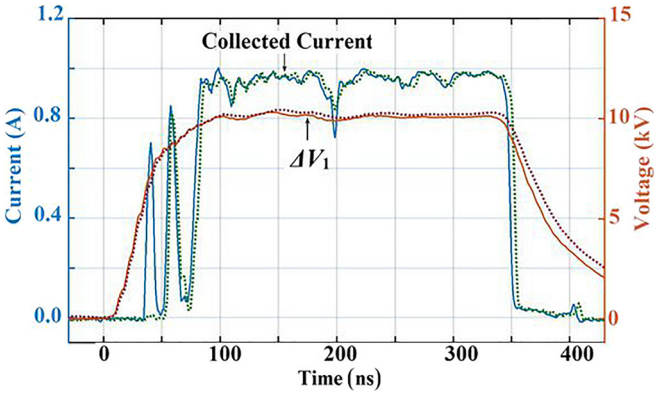

FIG. 6. Two registered traces of ΔV_1 and the current collected on the FC for $\Delta V_2 = -9$ kV and $\Delta V_3 = 9$ kV.

the FC for two different shots taken for the same conditions. Most of the features of the waveforms apart from one of the two current peaks detected during the voltage rise time recur. All other shots for the same parameters showed almost identical features.

As the voltage increases in the C1–A1 gap during the rise time, the emitted electrons gain an increasing energy, but since ΔV_2 is fixed, these electrons do not reach C_2 before the energy reaches $\sim e\Delta V_2$. Thus, a charge cloud containing electrons with different time dependent energies forms in the triode C_1–A_1–C_2 which can affect both the emission from the cathode and the reflection from C_2. This phenomenon can be responsible for the peaking seen during the rise time. We shall test this assumption in Sec. IV. The voltage ΔV_1 in Fig. 6 after the rise time along the plateau has long period small oscillations which could result in some of the small features seen in the current. Note that after the initial time, the entire current is transmitted to the FC without bunching.

Next, we decrease ΔV_3 ($\Delta V_3 > 0$) attempting to get to a point where gap C_2-A_2 becomes over-injected, causing the system to self-oscillate and transmit periodic electron bunches towards the Faraday cup. In Fig. 7, one can see typical waveforms of ΔV_1 and the electron beam current collected on the Faraday cup. Indeed, decreasing ΔV_3, which dictates the SCL current amplitude in gap C_2–A_2, leads to the appearance of modulations in the electron beam current registered by the Faraday cup. The most pronounced modulations occur at $\Delta V_3 = 0.5$ kV. One should note that the value of the voltage ΔV_1 in the C_1-A_1 gap is measured within an error of $\sim\pm 3\%$, which affects the relative values of ΔV_2 and ΔV_3 too. Therefore, when the experiment and the simulations (Sec. IV) are compared, only the trend in the behavior of the results should be considered.

These experiments demonstrate that the value of ΔV_3 affects the behavior of the system as expected from our over-injection model. The current modulation obtained is reproducible and so is the spotty pattern of the emitting surface of the dispenser cathode. We think that this spotty pattern leads to a non-uniform charge distribution in the various gaps of the tetrode, which strongly affects the dynamics of the space charge in the tetrode.

IV. PIC SIMULATIONS OF THE ELECTRON DYNAMICS IN THE EXPERIMENTAL SETUP

The finite radius cylindrical cathode has a sharp edge where the electric field and current emission are enhanced. We decided not to

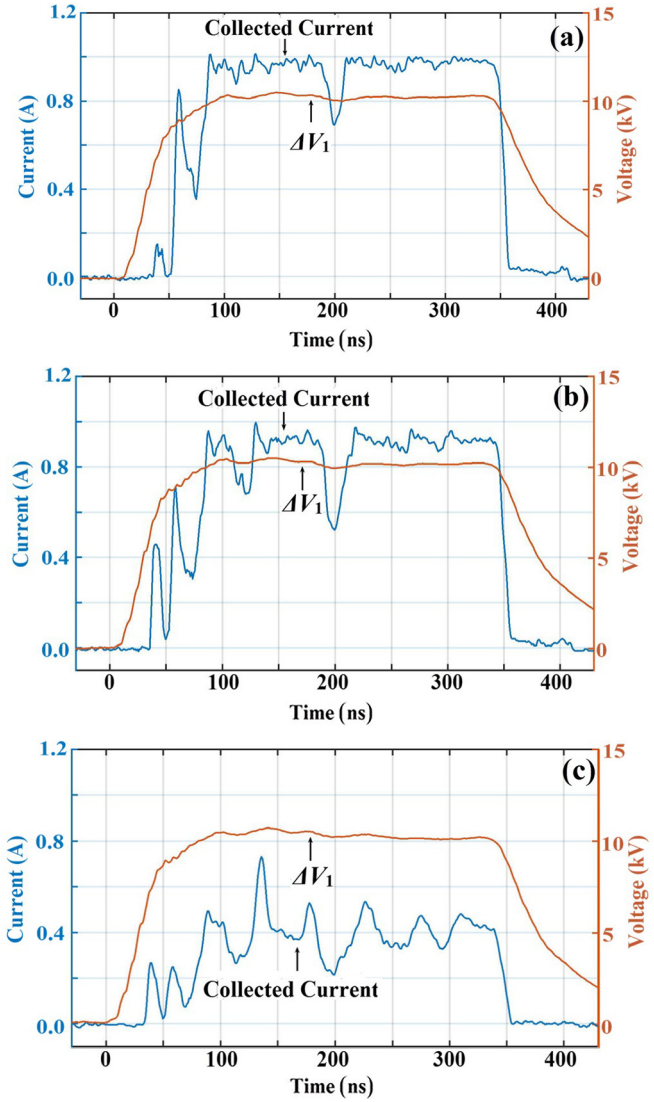

FIG. 7. Typical waveforms of ΔV_1 and the electron beam current collected on the FC for $\Delta V_2 = -9$ kV and (a) $\Delta V_3 = 2.5$ kV, (b) $\Delta V_3 = 2$ kV, and (c) $\Delta V_3 = 0.5$ kV.

use conventional field shaping techniques to reduce this effect because this would reduce the current considerably. Therefore, the 1 A emitted electron current has a radial current density distribution. Using the MAGIC-PIC[11] code, we calculate the SCL current of such an arrangement, in the presence of a constant axial magnetic field of 0.54 T, to be 5.67 A. A total current of 1 A emitted by a thermionic cathode is far below this value. In all our simulations, the 94% transmission Mo grids A_1, C_2, and A_2 emit scattered and impact ionization electrons which the PIC code calculates. We first assume that the voltage in all the gaps is constant at the values seen in Fig. 1, that is, the voltage in gap C_1-A_1 is switched on suddenly. In Fig. 8, the emitted current and the current collected on the Faraday cup as a function of time are drawn. The emitted current has a constant value of $\sim$1 A, but starting at $\sim$25 ns, every $\sim$1.6 ns, the cathode emits less current for a short time. The

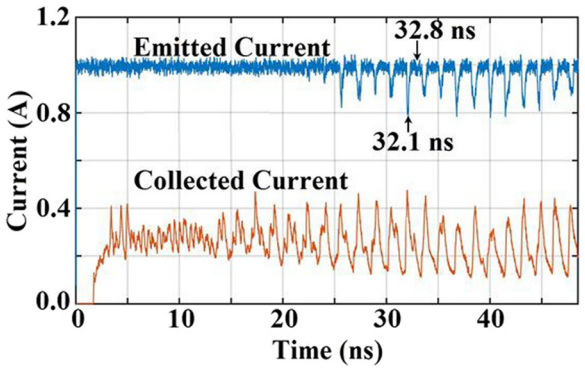

FIG. 8. The current emitted from the thermionic cathode and that collected on the Faraday cup for the voltage values in Fig. 1 and ΔV_1 rising suddenly at $t = 0$.

current collected on the Faraday cup is ∼0.1–0.45 A arriving in bunches, which start earlier than those seen emitted from the cathode with the same periodicity.

In Fig. 9(a), the accumulated electron charge in each gap of the tetrode C_1-A_1-C_2-A_2 is drawn. The charge in each gap of the triode increases, while it oscillates between the gaps with increasing amplitude. The time when the charge reaches its almost constant level at ∼25 ns coincides with the start of oscillations in the emitted current in Fig. 8.

The cathode emission fills the triode with charge which drains out in part depending on the value of ΔV_3. When this value is low, as is for the case discussed, a VC forms, first at the cathode end (C_2) of the C_2–A_2 gap, the result of over injecting this gap which we consider to be the "diode." This VC releases its excess charge in bunches flowing downstream towards the FC starting as early as ∼10 ns [Fig. 9(a)] and also charge bunches flowing through grid C_2 upstream until the entire triode becomes over-charged (∼25 ns) when the emission from the cathode C_1 is affected. ΔV_3 can be increased to a value where bunching and oscillations stop as seen in Fig. 9(b) for 4 kV. In Fig. 9(c), the charge accumulated in the gaps of the C1-A1-C2 triode of only the scattered and secondarily emitted electrons resulting from the impact with the grids for $\Delta V_3 = 0.1$ kV is drawn. The contribution of the scattered electrons during our simulation time is small and has little effect on the overall electron dynamics. Most of the electrons resulting from the scattering with grid C_1 remain and keep oscillating in the C_1-A_1-C_2 triode. Their charge increases very slowly as long as the main current flows. The scattering of electrons with grid C_2 is not a source of more charge because the impacting electrons have low energy. The scattered electrons from grid A_2 flow towards the FC, so the charge accumulated in the C_2-A_2 gap is negligible (∼3 pC).

In Fig. 10, the phase space of electrons of different origins is drawn for the time points designated in Fig. 8. Most of the current is carried by the electrons emitted on the cathode face and edge (blue). At 32.1 ns [Fig. 10(a)], the electron cloud is large near the cathode C_1 and screens the emission (Fig. 8). At 32.8 ns [Fig. 10(b)], the majority of the electron cloud is near C_2, a VC forms in gap C_2-A_2, and a bunch is released towards the Faraday cup. At the same time, the cathode emits again 1 A (Fig. 8). Note in Fig.10 that when the axial momentum, p_z, is negative, electrons return upstream and two VCs develop, at the beginning of the C_2–A_2 gap and at the end of the A_1–C_2 gap, each a few mm long.

Finally, in Fig. 11(a), the current collected on the Faraday cup for the different values of ΔV_3 is depicted. One can see that the value of ΔV_3 controls the electron dynamics, and for this reason, we consider gap C_2-A_2 a diode which becomes persistently over-injected for low enough ΔV_3. Namely, for $\Delta V_3 < 4$ kV, the current collected by the Faraday cup is unstable. When unstable, it starts off with the fast oscillations of ∼1.8 GHz which develop into the slow oscillations of ∼0.6 GHz discussed above (see Fig. 9). The scattered and secondary electron current collected on the FC is small and does not contribute to the collected electron dynamics [Fig. 11(b)].

In Fig. 12, we draw the charge accumulated in a 2.2 mm long interval containing the VC at the beginning of the C_2–A_2 gap. We assume that the fast oscillations in the time interval up to ∼15 ns in Fig. 12 are VC charge oscillations. We estimate the maximum electron density in the VC to be $\sim 3 \times 10^{10}$ cm^{-3}, which results in a plasma electron frequency of ∼1.5 GHz which is to be compared to ∼1.8 GHz, the fast oscillation frequency seen during the initial time period.

To estimate the frequency of the slower oscillation [∼0.6 GHz in Fig. 11(a)], we calculate the period of time for a single electron to traverse the C_2-A_1-C_2 route to be ∼1.27 ns which corresponds to ∼0.8 GHz. This value is higher than the observed frequency because it does not account for the effect of the accumulated charge in the triode.

The behavior described so far is similar to that presented in Ref. 10, apart from the period of the oscillations and the values of the currents and voltages because of the different conditions resulting from the cathode shape, dimensions, the voltage rise time, and electron collisions with the grids.

We now consider the effect of the rise time of the voltage applied on the dispenser cathode. We assume that the voltage in the C_1–A_1

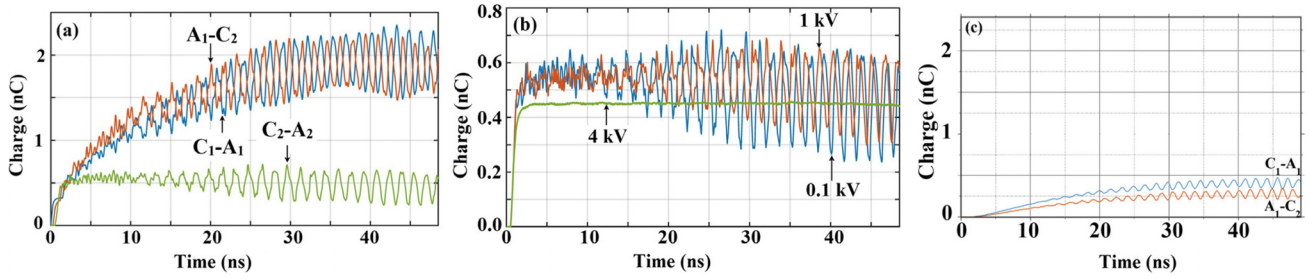

FIG. 9. (a) The accumulated charge in the three gaps of the tetrode C_1-A_1-C_2-A_2 for $\Delta V_3 = 0.1$ kV as a function of time and (b) the accumulated charge in gap C_2-A_2 vs. time for the increasing values of ΔV_3. (c) The same as (a), but only the scattered and secondary electrons are included.

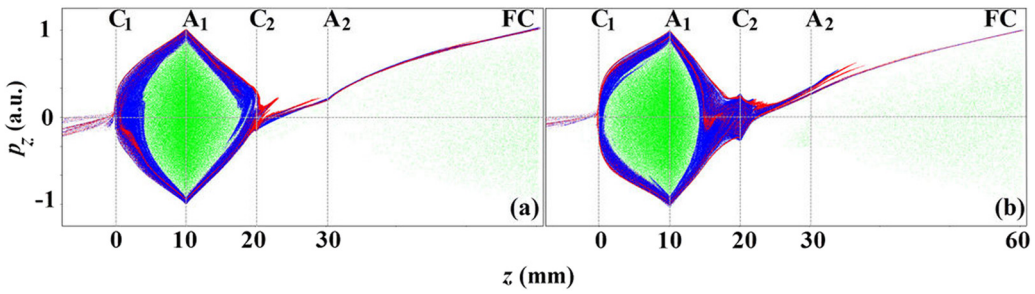

FIG. 10. Electron phase space at 32.1 (a) and 32.8 ns (b) (see Fig. 8). Electrons originate on the cathode face and edge (blue), the cathode side (red), and scattered and secondarily emitted from the grids (green).

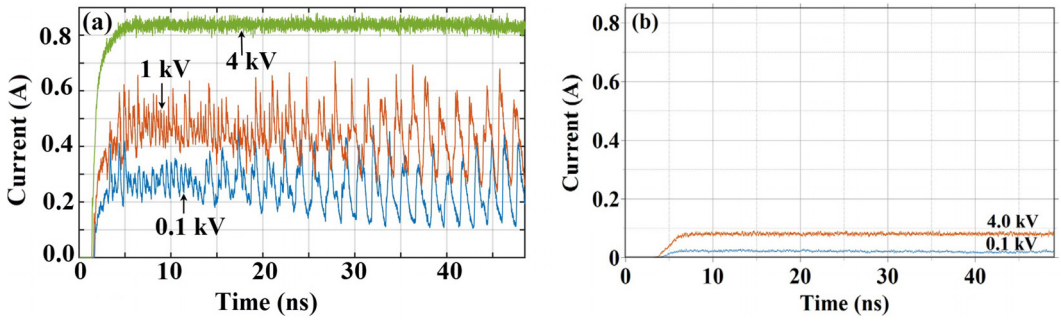

FIG. 11. (a) The current collected on the Faraday cup for the different values of ΔV_3. (b) Same as (a), but only the scattered and secondary electrons are measured.

gap rises in 20 ns and is constant in all other gaps in Fig. 1. We use the MAGIC-PIC code's thermionic emission model which applies the Richardson-Dushman equation to calculate the emitted electron current.

In Fig. 13, the voltage difference, ΔV_1, the emitted current, and the current collected on the FC are displayed. As the voltage rises, shown in Fig. 13, the emitted current rises too but only to a level of ~0.8 A which increases to almost the same oscillating structure, bound by the maximum current of 1 A as that seen in Fig. 8 starting at ~25 ns. Note that when the voltage rises suddenly (Fig. 8), the emitted current is constant up to ~25 ns. Here, the ~1.6 ns period oscillations of the emitted current of ~ 0.8 A start at ~15 ns, which become later bound by 1 A.

In Fig. 14, the phase space p_z vs. z in the triode is displayed at a time during the rise time of the voltage. The oscillating structure of the low energy electrons filling the gaps with space charge can be seen. We shall follow this space charge of low energy electrons formed during the rise time below.

In Fig. 15(a), the time dependence of the accumulated charge in the gaps C_1–A_1, A_1–C_2, and C_2–A_2 as a function of time is drawn. We see that the charge in gaps C_1–A_1 and A_1–C_2 rises up to ~18 ns when

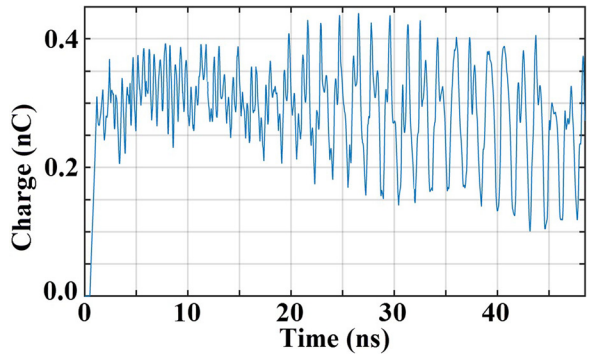

FIG. 12. Accumulated charge in the 2.2 mm interval at the beginning of the C_2–A_2 gap for $\Delta V_3 = 0.1$.

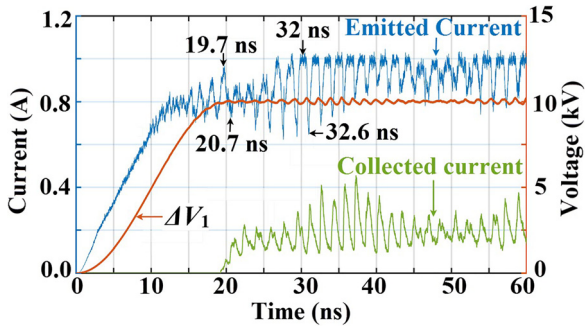

FIG. 13. ΔV_1, the emitted current, and the current collected on the FC as a function of time for the voltage values in Fig. 1 and ΔV_1 rising in 20 ns.

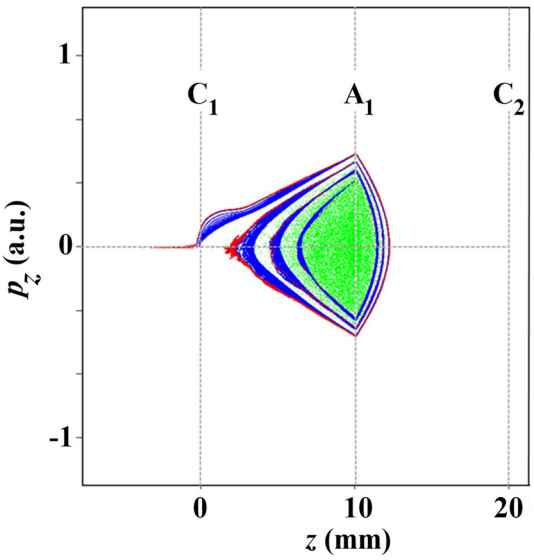

FIG. 14. Phase space of the electrons during the rise time at $t = 6.7$ ns. Electrons originating along the cathode face and edge (blue), along the side of the cathode (red), and those scattered or secondarily emitted from grid A_1 (green) are drawn.

it starts leaking out into gap C_2–A_2. Almost no charge oscillations are seen until the rise time ends, when first the amplitude of the oscillations increases in all three gaps and then decreases towards ~50 ns, while the charge in gaps C_1–A_1 and A_1–C_2 decreases as well. Then, the oscillations pick up again bound from above at the same level as the charge oscillations seen in Fig. 9(a) (when the charge there reaches a plateau in the absence of rise time electrons). In Fig. 15(b), the accumulated charge of only the rise time electrons in the three gaps of the tetrode is drawn. The charge of the rise time electrons disappears completely after ~40–50 ns. The restart of the same oscillatory behavior as that seen for sudden rise time coincides with the depletion of the rise time electrons. Unfortunately, we are unable to simulate for times above 50–60 ns because numerical noise starts to accumulate. The oscillatory behavior of the charge accumulated in the various gaps is reflected in the current collected on the Faraday cup (see Fig. 13). The contribution of the scattered and secondary electrons [Fig. 15(c)] is similar to that when the cathode is switched on suddenly [Fig. 9(c)].

Figure 16(a) is equivalent to Fig. 11(a) but for a 20 ns rise time in ΔV_1. For $\Delta V_3 = 1$ and 0.1 kV, the oscillatory behavior in Fig. 16(a) becomes, in time, the same as that seen in Fig. 11. For $\Delta V_3 = 1$ kV, these oscillations start earlier (~40 ns) because the higher voltage drains out the accumulated rise time electrons charge faster. Then, for 4 kV, in contrast to Fig. 11, although the average current is almost the same, it is not constant, but smaller amplitude oscillations are retained. This can be explained by the fact that although most rise time electrons have been drained out, the effect of their charge on the dynamics of the post-rise time electrons has not cleared out during the simulation time. This is seen in Fig. 17 where the post rise time electrons are still reflected in the triode and VCs form.

Figure 16 should be compared to the experimental results in Fig. 7. For both, we see that as ΔV_3 is decreased, the average transmitted current becomes smaller and the slower oscillations set on. In the

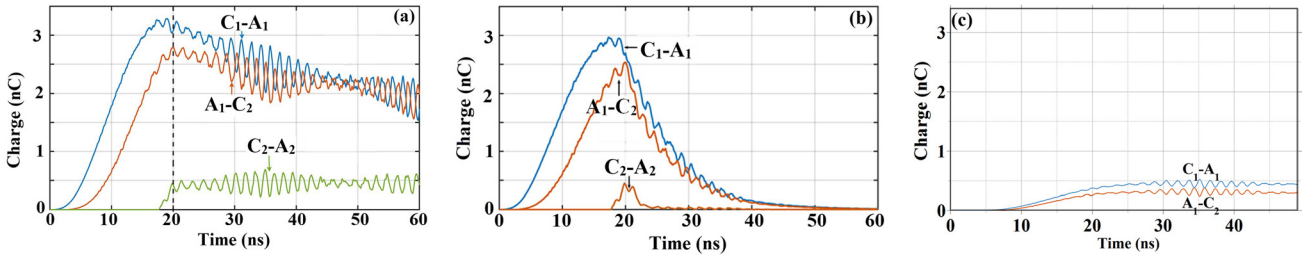

FIG. 15. (a) The accumulated electron charge in the three consecutive gaps of the tetrode as a function of time. (b) Same as (a), but only the charge of the electrons emitted during the rise time is included. (c) Same as (a), but only the scattered and secondary electrons are included. (The charge of these electrons in gap C_2-A_2 is negligible and is not drawn.)

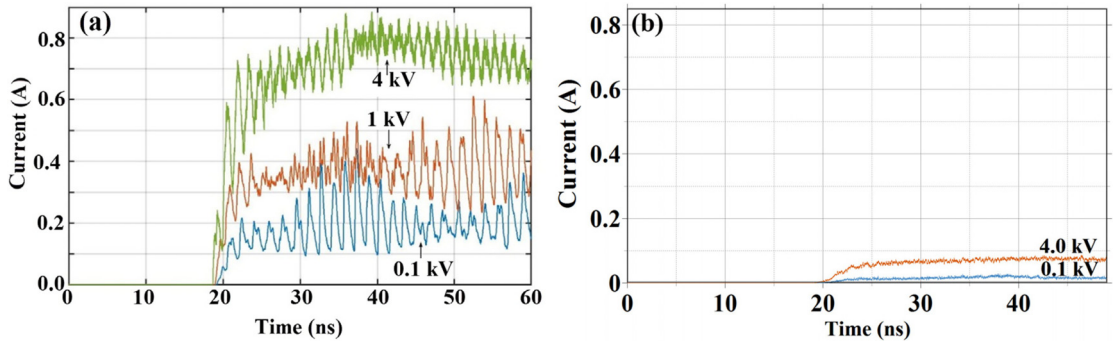

FIG. 16. The time dependence of the current collected on the Faraday cup for the increasing values of ΔV_3.

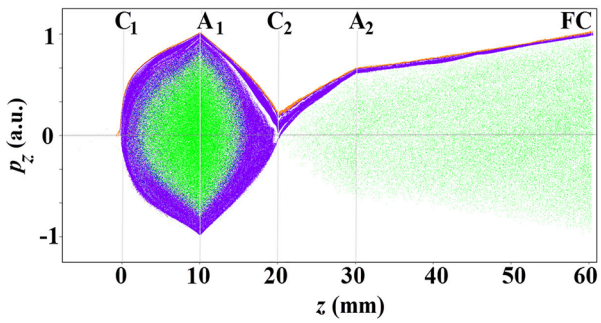

FIG. 17. Phase space of all electrons at $t = 50$ ns for $\Delta V_3 = 4$ kV. The purple electrons are emitted from the cathode face and edge and the orange colored electrons from the side of the cathode both post rise time. The green colored electrons are scattered or secondarily emitted from the grid, and the other colored electrons are a few remaining rise time electrons.

simulations, the characteristic frequency of these is ∼1.8 GHz, whereas in the experiment, these are very slow modulations rather than regular oscillations [Fig. 7(c)]. We attribute this behavior to the spotty emission characteristics of the dispenser cathode which affects the space charge distribution in the system and consequently the dynamics of this highly non-linear system.

V. SUMMARY

We have experimentally demonstrated that our scheme proposed in Ref. 10 to produce a modulated electron beam by over-injecting a diode is feasible, but we have not been able to reproduce the periodic behavior with the expected frequency because our dispenser cathode did not emit uniformly over its entire surface. By PIC simulations, we have shown the complications introduced by having a finite area cathode, scattering from finite transmission grids, and the voltage applied on the cathode rising during a finite time.

We show that in spite of the fact that these complications have a serious effect on the expected results, it is still possible to obtain a periodic electron source by lowering the value of ΔV_3. To improve our experimental results presented here, we intend to acquire a cathode with a uniform emission pattern over its surface, and we shall attempt to reduce the rise time significantly so that there will be a little low energy charge accumulation and improve the accuracy of ΔV_1.

ACKNOWLEDGMENTS

The authors are grateful to Svetlana Gleizer, Irena Feldman, and Eugene Flyat for their invaluable technical assistance.

REFERENCES

[1]P. Zhang, Á. Valfells, L. K. Ang, J. W. Luginsland, and Y. Y. Lau, Appl. Phys. Rev. **4**, 011304 (2017).
[2]C. K. Birdsall and W. B. Bridges, J. Appl. Phys. **32**, 2611 (1961).
[3]W. B. Bridges and C. K. Birdsall, J. Appl. Phys. **34**, 2946 (1963).
[4]Á. Valfells, D. W. Feldman, M. Virgo, P. G. O'Shea, and Y. Y. Lau, Phys. Plasmas **9**, 2377 (2002).
[5]J. R. Harris and P. G. O'Shea, IEEE Trans. Electron Devices **53**, 2824 (2006).
[6]J. G. Neumann, J. R. Harris, B. Quinn, and P. G. O'Shea, Rev. Sci. Instrum. **76**, 033303 (2005).
[7]K. Tian, R. A. Kishek, P. G. O'Shea, R. B. Fiorito, D. W. Feldman, and M. Reiser, Phys. Plasmas **15**, 056707 (2008).
[8]D. H. Dowell, S. Joly, A. Loulergue, J. P. de Brion, and G. Haouat, Phys. Plasmas **4**, 3369 (1997).
[9]A. Pedersen, A. Manolescu, and Á. Valfells, Phys. Rev. Lett. **104**, 175002 (2010).
[10]J. G. Leopold, M. Siman-Tov, A. Goldman, and Ya. E. Krasik, Phys. Plasmas **24**, 073116 (2017).
[11]B. Goplen, L. Ludeking, D. Smith, and D. Warren, Comput. Phys. Commun. **87**, 54 (1995).